

MODELING OF THE FREQUENCY DEPENDENCE OF THE CELLO PHOTO CURRENT FOR INCREASING MEASUREMENT SPEED AND IDENTIFICATION OF DEFECT TYPES

A. Schütt, S. Keipert, J. Carstensen, H. Föll
Institute for Materials Science, Faculty of Engineering, Christian-Albrechts-University of Kiel
Kaiserstr. 2, D-24143 Kiel, Germany

ABSTRACT: Combining the conventional CELLO (solar CELI Local characterization) technique with impedance analysis allows to identify locally distributed solar cell properties like photocurrent, lifetime, diffusion constant of minorities, surface recombination velocity on the back side, etc., due to their individual frequency response behavior (see section 2). Data for a range of frequencies are fitted to a model function (see section 3.1) at every pixel of CELLO current response maps obtained under short circuit conditions. The model function contains components describing the local solar cell parameters of interest as well as CELLO set up parameters that influence the frequency response. First impedance fit results are presented (see section 3.2) and compared with conventional CELLO results (see section 3.3).

Keywords: defects, characterization, modeling

1 MEASUREMENT TECHNIQUE CELLO

1.1 Introduction

The CELLO (solar CELI LLocal characterization) technique allows to measure all parameters of the equivalent circuit of a solar cell locally, fast, and non-destructive [1, 2]. The technique analyses the current or voltage response of a globally illuminated solar cell to local disturbances induced by LASER beam sinusoidally modulated with one frequency. The linear current or voltage response together with the phase change can be measured very precisely by lock-in technique at different points along the IV-curve. The obtained data, i.e. amplitude and phase shift maps, then allow to determine desired local parameters like serial resistances, shunts or the photocurrents [3, 4]. For a quantitative analysis of the DC conditions the modulation frequency of the laser beam up to now has been chosen low enough to obtain a neglectable phase shift, but as high as possible to gain measurement speed [5]. A new approach to get more local solar cell information in the same measurement time is to combine the conventional CELLO technique with impedance analysis.

1.2 Impedance analysis

Impedance spectroscopy (IS) is a standard technique in electrochemistry; a more recent development is FFT IS [6]. Basically, the response of an “electrochemical” system to a multifrequency perturbation signal is analyzed by fitting the recorded impedance data to a model; often in the form of an equivalent circuit. The physical meaning of the model is then analyzed in a second step to identify frequency dependent phenomena. The technique is easily transferred to solar cells. It will be shown that understanding the CELLO photo current response $dI_{sc}(\omega)$ under short circuit conditions at higher (cycle) frequencies ω allows to extract a number of local parameters as, e.g., local defect types, by their typical frequency response, as will be demonstrated in the following section.

2 FREQUENCY DEPENDENCE OF PHASE SHIFT

To investigate the frequency dependence of the amplitude and phase shift, CELLO maps of dI_{sc} are recorded at 14 different frequencies for a section of a standard mc Si solar cell. Fig. 1 displays the frequency response by using the mean values for each map at a certain frequency. For common dI_{sc} CELLO measurements a frequency of around 8000 Hz would be chosen, to approximate DC conditions (small phase shift) and to maximize measurement speed. Resonance behavior (see section 3.1 and Eq. (1)) can be observed at the amplitude response (cf. Fig. 1: Peak at around 30000 Hz). At higher frequencies the low-pass behavior (see section 3.1 and Eq. (2)) of the system dominates the response and the amplitude decreases to nearly zero.

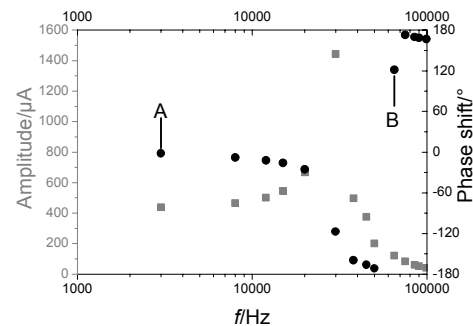


Figure 1: Frequency response of a multicrystalline Si solar cell. Mean values of the amplitude maps are grey squares. Mean values of the phase shift maps are black circles. Phase shift maps of the labels A and B are shown in Fig. 2b) and c).

A representative dI_{sc} map taken at 3007 Hz (Point A in Fig. 1) is given in Fig. 2a); it approximates the DC case. Maps at higher frequencies look rather similar – only their mean values change significantly. Fig. 2b) and Fig. 2c) show the phase shift maps at 3007 Hz and 65.007 Hz (points A and B in Fig. 1). There are significant differences between these two maps, and, on hindsight, areas of the missing BSF (cf. Fig. 2c mark A), an increased serial resistance due to a broken grid finger (cf. Fig. 2c mark B), and areas of reduced lifetime (cf.

e.g. Fig. 2c mark C) can be identified. These maps already demonstrate that different defect types may have specific “frequency fingerprints”, which might allow quantitative identification. Experiments with Cz Si solar cells (not presented here) show that this is also true for the doping concentration, because the typical rings of varying doping concentration n are only visible at lower frequencies.

In order to separate the various local solar cell parameters and defect types by their characteristic frequency behavior, an impedance fit algorithm has been developed, based on a complete theory of carrier generation and transport in the system under investigation.

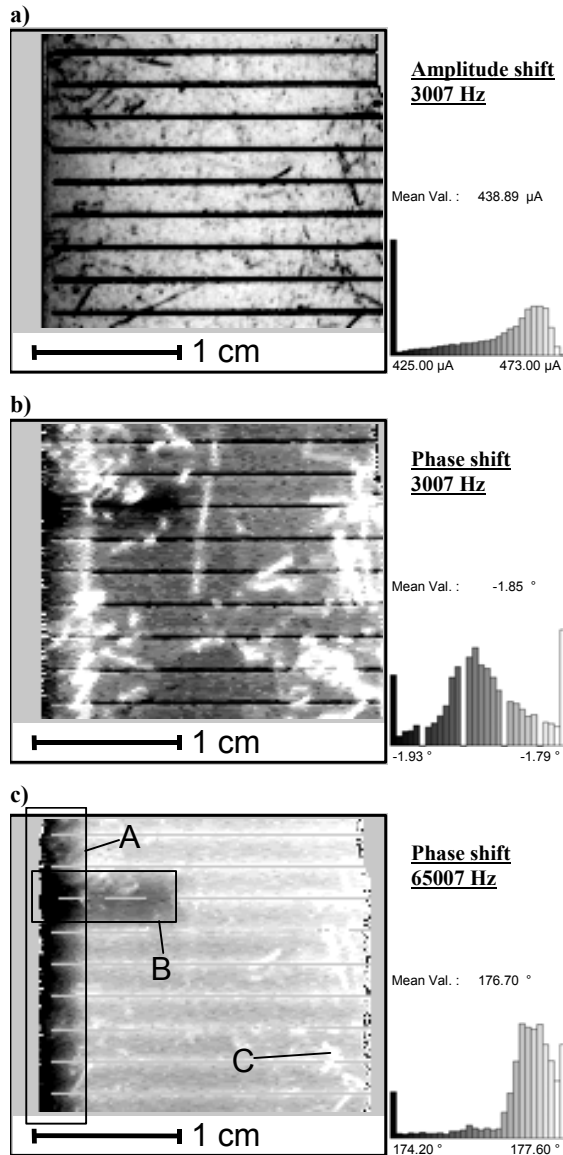


Figure 2: CELLO dI_{sc} maps for a part of a mc Si solar cell. a) amplitude at 3007 Hz, b) phase shift at 3007 Hz, c) phase shift at 65007 Hz. Areas of missing BSF (A), increased serial resistance due to a broken grid finger (B), and of reduced lifetime at grain boundaries (C) can be tentatively identified by comparing the phase shift maps.

3 IMPEDANCE FIT UNDER SHORT CIRCUIT CONDITIONS

3.1 Model and theoretical impedance

The amplitude and the phase shift can be expressed as complex impedance $Z(x,y,\omega)$; which is the product of three independent impedances: Z_{Sys} = (damped) resonance component of the measurement system; Z_{RC} = RC component of the electrical circuit; Z_{SC} = time dependent solution of the diffusion equation for the solar cell.

Z_{Sys} is given by Eq. (1). It is caused by the interplay of the potentiostat/galvanostat and the solar cell due to the voltage feedback [7] and actually dominates the spectra (cf. Fig. 4.) The attenuation constant K_F and the resonance frequency ω_0 thus are not local solar cell parameters but (uninteresting) “set up” constants.

$$Z_{\text{Sys}} = \frac{1}{1 - \left(\frac{\omega}{\omega_0}\right)^2 + iK_F\omega} \quad (1)$$

Z_{RC} is sufficiently well described by the simple relaxation approach [7]

$$Z_{RC} = \frac{1}{1 + i\omega RC} \quad (2)$$

with RC = low-pass time constant due to RC elements between illumination spot and reference electrode.

The solution Z_{SC} of the diffusion equation is given by the product of $Z_{SC} = Z_{SC1} \cdot Z_{SC2}$ according to

$$Z_{SC1} = qF(1-R) \frac{1}{1 - \left(\frac{A}{\alpha}\right)^2} \quad (3a)$$

$$Z_{SC2} = \frac{\frac{A}{\alpha} \left(1 - \frac{S_B}{D\alpha}\right) - \tanh(dA) \left(\left(\frac{A}{\alpha}\right)^2 - \frac{S_B}{D\alpha}\right)}{\frac{A}{\alpha} - \tanh(dA) \frac{S_B}{D\alpha}} \quad (3b)$$

with

$$A = \sqrt{\frac{1}{L^2} + \frac{i\omega}{D}} = \frac{1}{\sqrt{D}} \sqrt{\frac{1}{\tau} + i\omega} \quad (3c)$$

and

q : elementary charge.

F : photocurrent per area, i.e. ratio between LASER intensity and photogenerated charge carriers.

R : reflectivity.

α : absorption coefficient of light in Silicon.

D : diffusion constant of the minorities.

S_B : surface recombination velocity on the back side of the solar cell.

d : thickness of the solar cell.

ω : modulation frequency.

τ : lifetime of minorities.

The solution given is for a standard mc solar cell; for different types it may have to be modified.

3.2 First results of impedance fit

A part of a 10 cm x 10 cm mc Si solar cell is investigated. The conventional CELLO serial resistance map [3] is shown in Fig 3. For the impedance analysis 12 CELLO dI_{sc} maps of various frequencies are recorded successively. One pixel of each map contains amplitude and phase shift data. Using the proposed model function $Z(x,y,\omega)$, the frequency response of every pixel can be fitted quite well. This is illustrated for two pixels with different contrast in Fig. 2. In the example given the first pixel has a quite high serial resistance, contrary to the second one. Fig. 4 presents the frequency response (symbols) of these two pixels and the fit (line between fit points). The fit shows very good agreement with the measured data, but not much difference between the pixels. This is simply due to the large scale needed to accommodate the whole curves; on a smaller scale (see insets), the differences are clear and correspond (in %) to the scales in Fig. 2.

All pixels are fitted using $Z(x,y,\omega)$ knowing that the parameters α and d are constants. The resulting maps of the fit parameters shown in Fig. 5 are: (Photocurrent) · (1-reflectivity), τ , RC , D , S_B , K_F , and ω_0 . The coefficient of variation for the resulting K_F and ω_0 maps are 0,8% and 0,02%, respectively, and thus very small proving that they are not local parameters of the solar cell. Using just the mean values of K_F and ω_0 considerably improves the fitting speed and stability for the remaining parameters of interest. The resulting maps are presented in Fig. 5. Note that the numbers obtained are all fully compatible with what is known for this cell type; see section 3.3. Outstanding features of this new analyzing tool are:

- 1) All local parameters described in the model function can be determined and mapped under dI_{sc} conditions.
- 2) In particular, S_B and D can now be mapped for the first time.
- 3) Contrary to the LBIC technique no independent reflection measurement is needed to determine the photocurrent (and all other parameters).

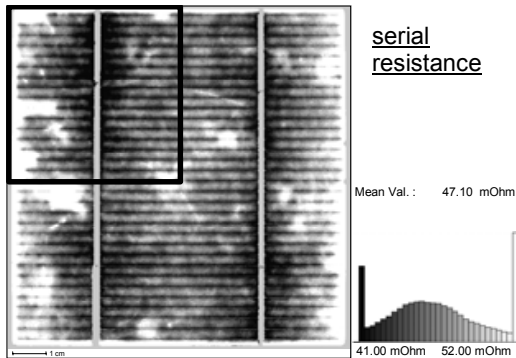


Figure 3: Conventional CELLO serial resistance map [3]. The marked section is investigated by the impedance fit.

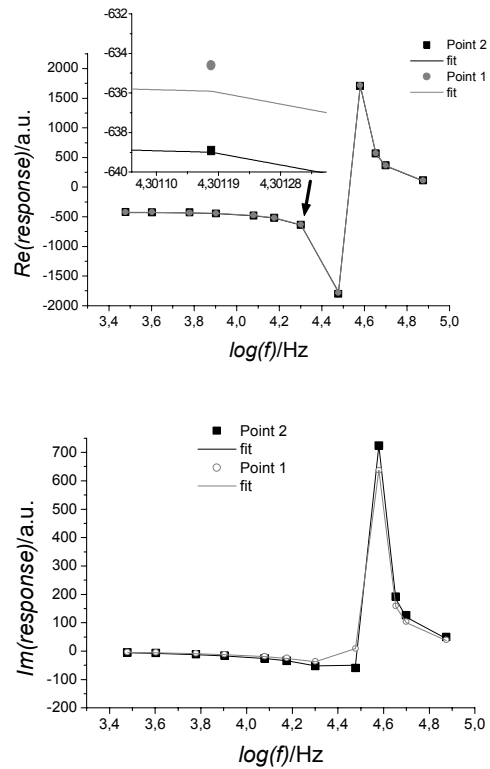


Figure 4: Frequency response of the real and imaginary part of the impedance for a mc Si solar cell at two different pixels. For details see text.

3.3 Consistency check of first impedance fit results and secondary maps

First, the mobility μ is calculated by using the Einstein relationship and the D -map, giving perfectly reasonable values (not shown here). Second, the local doping concentration n is derived from the mobility by well known relations and shown in Fig 6a. The local doping concentration then is used to calculate a local capacitance C_{Calc} . This allows to obtain a R_{Calc} map from the RC -map in Fig. 5c) by dividing by C_{Calc} ; the resulting map is shown in Fig. 6b. This map shows quite good agreement with the conventional CELLO serial resistance map in Fig. 3) and thus demonstrates the good quality of the fit. However, the still visible grain boundary structure indicates that some assumptions of the model may be too simple. This is also a possible explanation for the relatively large range of the doping concentration variation found in Fig. 6a).

4 SUMMARY AND OUTLOOK

4.1 Summary

- The frequency response of I_{SC} contains local information about all important solar cell parameters.
- Parameters often show specific frequency “fingerprint” which allows to directly identify typical defects.
- A theoretical understanding of the frequency response allows to map all relevant parameters.
- A CELLO like set-up (i.e. with a feedback loop) always behaves like a combination of low pass filter and a attenuated resonance circuit that must be included in any analysis

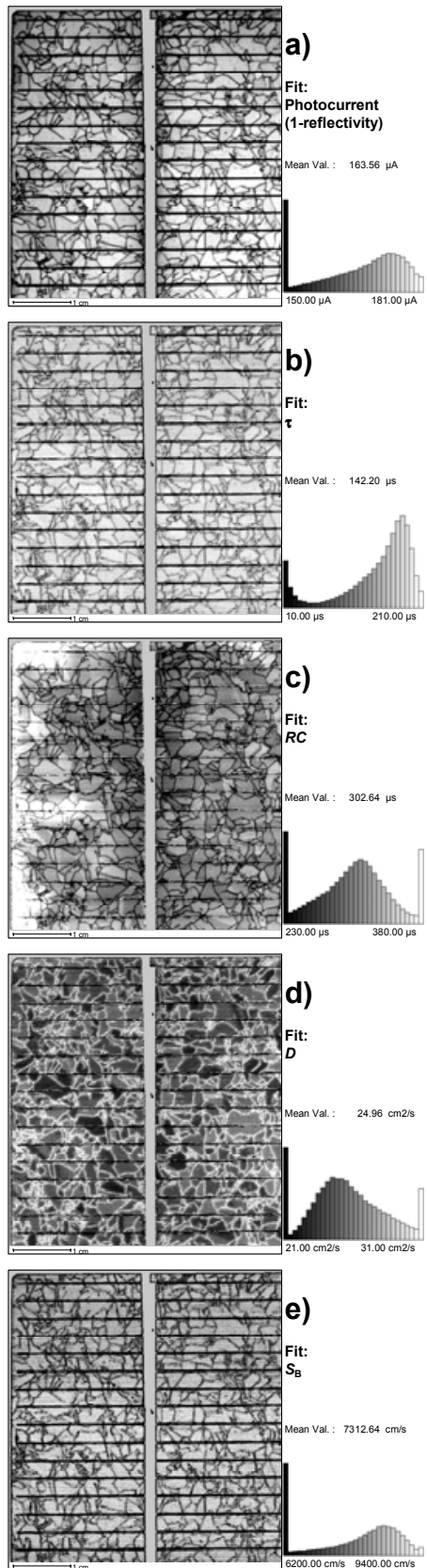


Figure 5: Fitparameter maps of a) Photocurrent-(1-reflectivity); b) τ ; c) RC; d) D; e) S_B . All numbers are found within a reasonable range.

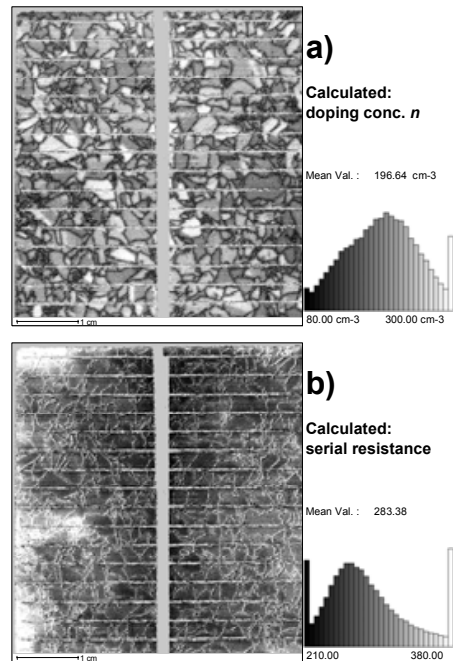


Figure 6: Secondary maps. a) doping concentration n ; b), and serial resistance map R_{Calc} .

4.2 Outlook

An FFT set up for recording the frequency response added to CELLO will allow a multi frequency modulation containing up to 30 frequencies and real time extraction of the response at all frequencies. The measurement time per pixel then is limited by the smallest frequency employed, but much smaller than the serial procedure. In practice no limiting of the present CELLO speed is expected, but much more data will be collected.

4.2 References

- [1] J. Carstensen, G. Popkirov, J. Bahr, and H. Föll, in *Proceedings of the 16th European Photovoltaic Solar Energy Conference*, VD3.35, Glasgow (2000)
- [2] J. Carstensen, G. Popkirov, J. Bahr, and H. Föll, *Solar Energy Materials & Solar Cells* 76, 599 (2003)
- [3] J. Carstensen, A. Schütt, and H. Föll, in *Proceedings of the 22nd European Photovoltaic Solar Energy Conference*, 1CV.1.34, Milan (2007)
- [4] A. Schütt, J. Carstensen, and H. Föll, in *Proceedings of the 21th European Photovoltaic Solar Energy Conference*, 1BV.2.36, Dresden (2006)
- [5] J. Carstensen, A. Schütt, G. Popkirov, and H. Föll, in *Proceedings of the 21th European Photovoltaic Solar Energy Conference*, 2AO.3.4, Dresden (2006)
- [6] G.S. Popkirov, *Electrochimica Acta* 41(7/8), 1023 (1996)
- [7] S. Keipert, J. Carstensen, and H. Föll, *ECS Transactions*, 211th Meeting of The Electrochemical Society, Chicago 6(2), 387 (2007)